# Untangling First and Second Order Statistics Contributions in Multipath Scenarios

Corentin Lubeigt[a,b,*], Lorenzo Ortega[a,c], Jordi Vilà-Valls[b], Eric Chaumette[b]

[a] *TéSA, 7, Boulevard de la Gare, 31500, Toulouse, France*
[b] *ISAE-SUPAERO, 10, Avenue Edouard Belin, 31055, Toulouse, France*
[c] *IPSA, 40, Boulevard de la Marquette, 31000, Toulouse, France*

**Abstract**

In ranging-based applications, ignoring the presence of multipath often leads to a bias upon the estimated range, which actually originates from misspecified estimation problem because the assumed data signal model, here without multipath, is not equal to the true one. Such misspecification also results in an error covariance matrix around the biased estimates, so-called pseudotrue parameters, that differs from the Cramér-Rao bound applied to the true model. This error covariance matrix can be lower bounded by a misspecified Cramér-Rao bound (MCRB). In this work, a closed-form expression of the MCRB under multipath conditions is proposed, which only depends on the baseband signal samples and both delay, Doppler and complex amplitude pseudotrue parameters. These MCRB expressions are fundamental i) to understand and characterize the impact of multipath conditions when not taken into account, ii) for system/signal design, and iii) to derive new robust estimators. The proposed MCRBs are validated for a representative navigation signal, comparing the resulting bounds with the mean square error obtained by the misspecified maximum likelihood estimator with respect to the pseudotrue parameters.

*Keywords:* Delay/Doppler estimation, maximum likelihood, misspecified models, CRB, multipath.

## 1. Introduction

Multipath is still one of the most challenging propagation conditions in ranging-based systems, such as radar, sonar or Globlal Navigation Satellite Systems (GNSS) [1, 2]. Indeed, its environment specific behaviour and randomness are difficult to anticipate, and the corresponding system performance degradation difficult to counteract. Several multipath mitigation strategies have been developed in both communities, ranging from hardware, e.g., choke ring antennas, to software/algorithmic solutions, where the latter typically try to estimate the multipath contributions. In addition, the multipath mitigation problem may also impact the signal design, or the corresponding performance metrics on how robust a given signal might be. Overall,

*Corresponding author
*Email address:* corentin.lubeigt@tesa.prd.fr (Corentin Lubeigt)

for both system/signal design and the derivation of robust estimators, it is fundamental to have mathematical tools to understand and characterize the impact of such multipath conditions when not taken into account.

If one considers a nominal scenario (where multipath is not expected), or the use of low-cost receivers that can not afford a multipath mitigation engine (i.e., standard GNSS receivers), multipath directly leads to a ranging/positioning estimation performance degradation, induced by an estimation bias that the receiver does not take into account. Indeed, from a system model perspective, ignoring the possible presence of multipath implies to consider a line-of-sight (LOS) single source model instead of the true multi source signal. Such assumption is known as model misspecification, of interest in several disciplines.

The performance of misspecified estimators was first studied in [3, 4, 5], and the mathematical framework to link such performance to the corresponding lower bounds was recently introduced in [6, 7]. In particular, it was shown that the mispecified maximum likelihood (MML) estimator converges to a fix value that minimizes the Kullback-Leibler divergence (KLD) between the true data model and the misspecified probability density functions (PDFs). Moreover, when the number of data points or the signal-to-noise ratio (SNR) are large enough, its mean square error (MSE) converges to the so-called misspecified Cramér-Rao bound (MCRB) [6, 7, 8]. Consequently a MML estimator is said to be misspecified-unbiased and asymptotically efficient.

The MCRB definition under the Gaussian assumption [6, 7] can be seen as an extension of the Slepian-Bangs formulas [9], which allow to derive the Fisher information matrix for a given estimation problem. The standard Slepian-Bangs formulas (without mismatch) were the starting point to obtain closed-form CRB expressions for different joint delay-Doppler estimation problems: i) single source model [10], or ii) dual source model [11]. These compact CRB expressions were conveniently expressed as a function of the baseband signal samples, therefore being easy to implement and useful for a plethora of signals/applications. In this contribution we further study the delay/Doppler estimation problem, and complement the results in [10, 11] with the derivation of a delay/Doppler (misspecified) estimation closed-form MCRB expressions in the presence of a multipath. Such lower bound allows to properly characterize the performance of standard ranging-based systems/receivers not accounting for such propagation effect, which was not possible with the results available in the literature. The resulting compact expressions are validated by exploiting the asymptotic properties of the MML for a representative signal, namely, a GPS L1 C/A navigation signal [12].

## 2. True and Misspecified Signal Models

Consider the transmission of an electromagnetic wave, traveling at the speed of light $c$, from a transmitter to a receiver. In general, both transmitter and receiver are assumed to be in uniform linear motion such that the distance between them can be approximated by a first order distance-velocity model [13]:

$$d_{\text{transmitter} \rightarrow \text{receiver}} = c\tilde{\tau}(t) \approx d + vt, \text{ and } \tilde{\tau}(t) \approx \tau + bt, \ \tau = \frac{d}{c}, \ b = \frac{v}{c}, \tag{1}$$

where $d$ is the absolute distance between the two objects at time $t = 0$, $v$ is the radial velocity between them, $\tau$ is the time-delay due to the propagation path and $(1 - b)$ is the dilatation induced by the Doppler effect. The electromagnetic wave is assumed to be a band-limited signal $s(t)$, with bandwidth $B$, transmitted over a carrier frequency $f_c$, which covers several applications of interest. This signal can be expressed as

$$s(t) = \sum_{n=N_1'}^{N_2'} s\left(\frac{n}{F_s}\right) \mathrm{sinc}\left(\pi F_s\left(t - \frac{n}{F_s}\right)\right) \leftrightharpoons S(f) = \frac{1}{F_s} \sum_{n=N_1'}^{N_2'} s\left(\frac{n}{F_s}\right) e^{-j2\pi n \frac{f}{F_s}}, \quad -\frac{F_s}{2} \leq f \leq \frac{F_s}{2}, \tag{2}$$

where $F_s \geq B$ is the sampling frequency, $N_1', N_2'$ in $\mathbb{Z}$, $N_1' < N_2'$ and $\leftrightharpoons$ refers to the time-frequency pair.

### *2.1. True Signal Model*

Using (1), and assuming a direct (indexed 0) and a reflected (indexed 1) propagation paths, the dual source complex analytic signal at the output of the receiver's antenna can be expressed as

$$x_a(t) = d_a(t;\boldsymbol{\theta}_0) + d_a(t;\boldsymbol{\theta}_1) + w_a(t)\,,\; d_a(t;\boldsymbol{\theta}_i) = \rho_i e^{j\phi_{a,i}} s((1-b_i)(t-\tau_i)) e^{j\omega_c(1-b_i)t} e^{-j\omega_c\tau_i}\,, \tag{3}$$

with $w_a(t)$ a zero-mean white complex circular Gaussian noise, and for $i \in \{0,1\}$ $\tau_i$ is the time delay, $b_i$ is the Doppler coefficient and $\rho_i$, $\phi_{a,i}$ are the amplitude and phase of the complex coefficients induced by the propagation characteristics (fading, reflection, *etc.*), the polarization mismatches and the antenna gains. Under the narrowband signal hypothesis, the Doppler effect on the band-limited baseband signal $s(t)$ can be neglected: $s((1-b)(t-\tau)) \approx s(t-\tau)$ [1, ch.9]. Then, the baseband output of the receiver's Hilbert filter containing the LOS signal and the reflected signal can be approximated

$$x(t) \triangleq x_a(t)e^{-j\omega_c t} = d(t;\boldsymbol{\theta}_0) + d(t;\boldsymbol{\theta}_1) + w(t)\,,\; d(t;\boldsymbol{\theta}_i) \triangleq \rho_i e^{j\phi_i} s(t-\tau_i) e^{-j\omega_c b_i(t-\tau_i)}\,, \tag{4}$$

where $\omega_c = 2\pi f_c$ and, for $i \in \{0,1\}$, $\boldsymbol{\theta}_i^T = [\boldsymbol{\eta}_i^T, \rho_i, \phi_i]$, $\boldsymbol{\eta}_i^T = [\tau_i, b_i]$, $\rho_i > 0$ and $\phi_i = \phi_{a,i} - \omega_c(1+b_i)\tau_i$. Considering the acquisition of $N = N_2 - N_1 + 1$ ($N_1 \ll N_1', N_2 \gg N_2'$) samples at the sampling frequency $F_s = B = 1/T_s$, the discrete signal model yields to the following dual source conditional signal model (CSM)[11], $\mathbf{x} = \alpha_0\mathbf{a}_0 + \alpha_1\mathbf{a}_1 + \mathbf{w}$, $\mathbf{w} \sim \mathcal{CN}(0, \sigma_n^2\mathbf{I}_N)$, with, for $i \in \{0,1\}$, $\alpha_i = \rho_i e^{j\phi_i}$ and, for $n \in [N_1, N_2]$, $\mathbf{a}_i^T = \big(\ldots,\; s(nT_s - \tau_i)e^{-j\omega_c b_i(nT_s-\tau_i)},\; \ldots\big)$, $\mathbf{w}^T = (\ldots,\; w(nT_s),\; \ldots)$ and $\mathbf{x}^T = (\ldots,\; x(nT_s),\; \ldots)$. Consequently, the true data model PDF, noted $p_{\mathbf{x}}(\mathbf{x};\boldsymbol{\theta}_0,\boldsymbol{\theta}_1)$, is written as,

$$p_{\mathbf{x}}(\mathbf{x};\boldsymbol{\theta}_0,\boldsymbol{\theta}_1) = \mathcal{CN}(\alpha_0\mathbf{a}_0 + \alpha_1\mathbf{a}_1, \sigma_n^2\mathbf{I}_N). \tag{5}$$

### *2.2. Misspecified Signal Model*

As previously stated, standard receiver architectures do not account for the presence of possible multipath conditions, which reduces to consider a single source signal model. Following the same reasoning as for the true signal model, it is straightforward to express the misspecified signal model as a single source CSM, $\mathbf{x} = \rho_{pt}e^{j\phi_{pt}}\mathbf{a}_{pt} + \mathbf{w}$, $\mathbf{w} \sim \mathcal{CN}(0, \sigma_n^2\mathbf{I}_N)$, with, $\alpha_{pt} = \rho_{pt}e^{j\phi_{pt}}$ and, for $n \in [N_1, N_2]$,

$\mathbf{a}_{pt}^T = \left(\ldots,\ s(nT_s - \tau_{pt})e^{-j\omega_c b_{pt}(nT_s-\tau_{pt})},\ \ldots\right)$, where the subscript $pt$ refers to *pseudotrue*, which will necessarily depend on the true values $\boldsymbol{\theta}_0$ and $\boldsymbol{\theta}_1$, as discussed in the next section. Then, the misspecified data model PDF, noted $f_{\mathbf{x}}(\mathbf{x}|\boldsymbol{\theta}_{pt})$ is written as,

$$f_{\mathbf{x}}(\mathbf{x};\boldsymbol{\theta}_{pt}) = \mathcal{CN}(\alpha_{pt}\mathbf{a}_{pt}, \sigma_n^2\mathbf{I}_N), \tag{6}$$

where $\boldsymbol{\theta}_{pt}^T = [\boldsymbol{\eta}_{pt}^T, \rho_{pt}, \phi_{pt}]$ is the vector of pseudotrue parameters. See Table A.1 for a numerical example of true and pseudotrue values, which will be further studied in Section 5.

## 3. Mismatched Maximum Likelihood Estimator

### *3.1. Definition of the MML Estimator*

Given the misspecified model (6), the MML is simply a single source ML estimator that aims at estimating the vector of pseudotrue parameters $\boldsymbol{\theta}_{pt}$ by maximizing the likelihood given the set of data $\mathbf{x}$. This maximization problem can be written as follows [14]:

$$\widehat{\boldsymbol{\eta}}_{pt} = \arg\max_{\boldsymbol{\eta}} \left|R_{\mathbf{x},\mathbf{a}}(\boldsymbol{\eta})\right|^2 ,\ \widehat{\rho}_{pt} = \left|R_{\mathbf{x},\mathbf{a}}(\widehat{\boldsymbol{\eta}}_{pt})\right| ,\ \widehat{\phi}_{pt} = \arg\left(R_{\mathbf{x},\mathbf{a}}(\widehat{\boldsymbol{\eta}}_{pt})\right) ,\ R_{\mathbf{x},\mathbf{a}}(\boldsymbol{\eta}) = \frac{\mathbf{a}^H(\boldsymbol{\eta})\mathbf{x}}{\|\mathbf{a}(\boldsymbol{\eta})\|} , \tag{7}$$

with $R_{\mathbf{x},\mathbf{a}}(\boldsymbol{\eta})$ the normalized complex cross ambiguity function between the received signal $\mathbf{x}$ and a clean replica $\mathbf{a}$. Depending on the modulation used (BPSK or CBOC), the cross function can adopt different shapes [2, Sec. 4.3].

### *3.2. Properties and Applications*

In the case of a misspecified configuration, that is, in presence of a multipath, the estimator's output in (7) can be biased, see [15, Sec. 9.5.2] where this bias is illustrated for different signals. Indeed, it is well known that when the multipath excess delay with regard to the LOS signal delay $(\tau_0 - \tau_1)$ is small, the interference between both signals distorts the ambiguity function to be maximized, which in turn results in a biased LOS time-delay estimate. Similarly, if the difference between LOS and multipath Doppler frequencies is small, it can also lead to a bias on the estimated frequency.

Even if the MML appears to be biased with respect to (w.r.t.) the true LOS signal parameters, it has the property to be a misspecified-unbiased estimator of the pseudotrue parameters vector $\boldsymbol{\theta}_{pt}$ [7]. Moreover, its MSE asymptotically tends to the MCRB, which makes it an asymptotically efficient estimator of the pseudotrue parameters. Firstly, according to the MML property shown in [6] and [7], for the considered observation models (5) and (6):

$$\boldsymbol{\theta}_{pt} = \arg\min_{\boldsymbol{\theta}} \{D(p_{\mathbf{x}}\|f_{\mathbf{x}})\} \Leftrightarrow \begin{cases} \boldsymbol{\eta}_{pt} = \arg\max_{\boldsymbol{\eta}} \left\{\left|R_{\alpha_0\mathbf{a}_0+\alpha_1\mathbf{a}_1,\mathbf{a}}(\boldsymbol{\eta})\right|^2\right\} \\ \alpha_{pt} = R_{\alpha_0\mathbf{a}_0+\alpha_1\mathbf{a}_1,\mathbf{a}}(\boldsymbol{\eta}) \end{cases} , \tag{8}$$

*Proof.* See the Technical Note [16, Sec. 2]. □

Even if there is no closed-form for (8), it can be easily evaluated numerically. Secondly, once the MCRB expression is obtained, a way to check its exactness is to run Monte Carlo simulations in order to compute the MSE of the MML estimator, and compare it to the MCRB. This is what is done in Sec. 5.

## 4. Closed-Form MCRBs for Delay/Doppler Estimation under Multipath

In [6], the MCRB have been described as an extension of the Slepian-Bangs formulas, which were then expressed as a combination of two information matrices in [7]: $\mathbf{A}(\boldsymbol{\theta}_{pt})$ and $\mathbf{B}(\boldsymbol{\theta}_{pt})$,

$$\mathbf{MCRB}(\boldsymbol{\theta}_{pt}) = \mathbf{A}(\boldsymbol{\theta}_{pt})^{-1}\mathbf{B}(\boldsymbol{\theta}_{pt})\mathbf{A}(\boldsymbol{\theta}_{pt})^{-1}\,, \tag{9}$$

$$\left[\mathbf{A}(\boldsymbol{\theta}_{pt})\right]_{p,q} = \frac{2}{\sigma_n^2}\mathrm{Re}\left\{(\delta\mathbf{a})^H\left(\frac{\partial^2\alpha_{pt}\mathbf{a}_{pt}}{\partial\theta_p\partial\theta_q}\right)\right\}\Bigg|_{\boldsymbol{\theta}=\boldsymbol{\theta}_{pt}} - \left[\mathbf{B}(\boldsymbol{\theta}_{pt})\right]_{p,q}\,, \tag{10}$$

$$\left[\mathbf{B}(\boldsymbol{\theta}_{pt})\right]_{p,q} = \frac{2}{\sigma_n^2}\mathrm{Re}\left\{\left(\frac{\partial\alpha_{pt}\mathbf{a}_{pt}}{\partial\theta_p}\right)^H\left(\frac{\partial\alpha_{pt}\mathbf{a}_{pt}}{\partial\theta_q}\right)\right\}\Bigg|_{\boldsymbol{\theta}=\boldsymbol{\theta}_{pt}}\,, \tag{11}$$

and $\delta\mathbf{a} \triangleq \alpha_0\mathbf{a}_0 + \alpha_1\mathbf{a}_1 - \alpha_{pt}\mathbf{a}_{pt}$ is the difference of the means between the true and the misspecified data models. The covariance matrices between both models are assumed to be equal.

### *4.1. Single Source Fisher Information Matrix*

In the matrix $\mathbf{B}(\boldsymbol{\theta}_{pt})$, one can recognize the Fisher Information Matrix of a single source CSM. A compact expression of this matrix, that depends only on the baseband signal samples, has recently been derived in [10] and is recalled hereafter for completeness,

$$\mathbf{B}(\boldsymbol{\theta}_{pt}) = \frac{2F_s}{\sigma_n^2}\mathrm{Re}\left\{\mathbf{Q}\mathbf{W}\mathbf{Q}^H\right\}\,,\ \mathbf{W} = \begin{bmatrix} w_1 & w_2^* & w_3^* \\ w_2 & W_{2,2} & w_4^* \\ w_3 & w_4 & W_{3,3} \end{bmatrix}, \tag{12}$$

with $\mathbf{Q}$ defined in (A.3), and the elements in $\mathbf{W}$ can be expressed w.r.t. the baseband signal samples,

$$w_1 = \frac{1}{F_s}\mathbf{s}^H\mathbf{s},\ w_2 = \frac{1}{F_s^2}\mathbf{s}^H\mathbf{D}\mathbf{s},\ w_3 = \frac{1}{F_s}\mathbf{s}^H\mathbf{V}^{\Delta,1}(0)\mathbf{s},\ w_4 = \frac{1}{F_s}\mathbf{s}^H\mathbf{D}\mathbf{V}^{\Delta,1}(0)\mathbf{s}, \tag{13}$$

$$W_{2,2} = \frac{1}{F_s^3}\mathbf{s}^H\mathbf{D}^2\mathbf{s},\ W_{3,3} = F_s\mathbf{s}^H\mathbf{V}^{\Delta,2}(0)\mathbf{s}, \tag{14}$$

where $\mathbf{s}$, the baseband samples vector, is defined in (A.17), $\mathbf{D}$ in (A.18), $\mathbf{V}^{\Delta,1}$ in (A.19) and $\mathbf{V}^{\Delta,2}$ in (A.20).

### *4.2. Model Mismatch Information Matrix*

The matrix $\mathbf{A}(\boldsymbol{\theta}_{pt})$ accounts for the model misspecification. Its elements can also be expressed in a compact form as a function of the baseband samples as,

$$\left[\mathbf{A}(\boldsymbol{\theta}_{pt})\right]_{p,q} = \frac{2F_s}{\sigma_n^2}\mathrm{Re}\left\{\left[\mathbf{Q}_q\right]_{p,.}\mathbf{W}^{\mathbf{A}}\right\} - \left[\mathbf{B}(\boldsymbol{\theta}_{pt})\right]_{p,q}\,, \tag{15}$$

where $\left[\mathbf{Q}_q\right]_{p,\cdot}$ is the $p$-th row of the matrix $\mathbf{Q}_q$, $\mathbf{W}^{\mathbf{A}}$ is defined as $\mathbf{W}^{\mathbf{A}} = \alpha_0 \mathbf{w}^{\mathbf{A}}(\boldsymbol{\eta}_0) + \alpha_1 \mathbf{w}^{\mathbf{A}}(\boldsymbol{\eta}_1) - \alpha_{pt}\mathbf{w}^{\mathbf{A}}(\boldsymbol{\eta}_{pt})$ and, for $k \in \{0, 1, pt\}$, $\Delta\tau_k = \tau_k - \tau_{pt}$, $\Delta b_k = b_k - b_{pt}$, $\mathbf{w}^{\mathbf{A}}(\boldsymbol{\eta}_k)$ is a six-element column vector whose components are

$$\mathbf{w}_1^{\mathbf{A}}(\boldsymbol{\eta}_k)^* = \frac{1}{F_s}\mathbf{s}^H\mathbf{U}\left(\frac{f_c\Delta b_k}{F_s}\right)\mathbf{V}^{\Delta,0}\left(\frac{\Delta\tau_k}{T_s}\right)\mathbf{s}\, e^{j\omega_c b_k\Delta\tau_k}, \tag{16}$$

$$\mathbf{w}_2^{\mathbf{A}}(\boldsymbol{\eta}_k)^* = \frac{1}{F_s^2}\mathbf{s}^H\mathbf{D}\mathbf{U}\left(\frac{f_c\Delta b_k}{F_s}\right)\mathbf{V}^{\Delta,0}\left(\frac{\Delta\tau_k}{T_s}\right)\mathbf{s}\, e^{j\omega_c b_k\Delta\tau_k}, \tag{17}$$

$$\mathbf{w}_3^{\mathbf{A}}(\boldsymbol{\eta}_k)^* = \frac{1}{F_s^3}\mathbf{s}^H\mathbf{D}^2\mathbf{U}\left(\frac{f_c\Delta b_k}{F_s}\right)\mathbf{V}^{\Delta,0}\left(\frac{\Delta\tau_k}{T_s}\right)\mathbf{s}\, e^{j\omega_c b_k\Delta\tau_k}, \tag{18}$$

$$\mathbf{w}_4^{\mathbf{A}}(\boldsymbol{\eta}_k)^* = \left(-\mathbf{s}^H\mathbf{U}\left(\frac{f_c\Delta b_k}{F_s}\right)\mathbf{V}^{\Delta,1}\left(\frac{\Delta\tau_k}{T_s}\right)\mathbf{s} + \frac{j\omega_c\Delta b_k}{F_s}\mathbf{s}^H\mathbf{U}\left(\frac{f_c\Delta b_k}{F_s}\right)\mathbf{V}^{\Delta,0}\left(\frac{\Delta\tau_k}{T_s}\right)\mathbf{s}\right) e^{j\omega_c b_k\Delta\tau_k}, \tag{19}$$

$$\begin{aligned}\mathbf{w}_5^{\mathbf{A}}(\boldsymbol{\eta}_k)^* = \Bigg(&-\frac{1}{F_s}\mathbf{s}^H\mathbf{U}\left(\frac{f_c\Delta b_k}{F_s}\right)\mathbf{V}^{\Delta,0}\left(\frac{\Delta\tau_k}{T_s}\right)\mathbf{s} - \frac{1}{F_s}\mathbf{s}^H\mathbf{D}\mathbf{U}\left(\frac{f_c\Delta b_k}{F_s}\right)\mathbf{V}^{\Delta,1}\left(\frac{\Delta\tau_k}{T_s}\right)\mathbf{s}\\ &+ j\frac{\omega_c\Delta b_k}{F_s^2}\mathbf{s}^H\mathbf{D}\mathbf{U}\left(\frac{f_c\Delta b_k}{F_s}\right)\mathbf{V}^{\Delta,0}\left(\frac{\Delta\tau_k}{T_s}\right)\mathbf{s}\Bigg)\, e^{j\omega_c b_k\Delta\tau_k},\end{aligned} \tag{20}$$

$$\begin{aligned}\mathbf{w}_6^{\mathbf{A}}(\boldsymbol{\eta}_k)^* = \Bigg(&-F_s\mathbf{s}^H\mathbf{U}\left(\frac{f_c\Delta b_k}{F_s}\right)\mathbf{V}^{\Delta,2}\left(\frac{\Delta\tau_k}{T_s}\right)\mathbf{s} - j2\omega_c\Delta b_k\mathbf{s}^H\mathbf{U}\left(\frac{f_c\Delta b_k}{F_s}\right)\mathbf{V}^{\Delta,1}\left(\frac{\Delta\tau_k}{T_s}\right)\mathbf{s}\\ &- \frac{(\omega_c\Delta b_k)^2}{F_s}\mathbf{s}^H\mathbf{U}\left(\frac{f_c\Delta b_k}{F_s}\right)\mathbf{V}^{\Delta,0}\left(\frac{\Delta\tau_k}{T_s}\right)\mathbf{s}\Bigg)\, e^{j\omega_c b_k\Delta\tau_k},\end{aligned} \tag{21}$$

*Proof.* See Appendix A and the associated Technical Note [16, Sec. 1]. □

## 5. Validation and Discussions

### 5.1. Methodology and Simulation Set-Up

In order to validate the MCRB expressions, the properties of the MML (see Sec. 3.2) are exploited. Indeed, the MML being an asymptotically efficient misspecified-unbiased estimator of $\boldsymbol{\theta}_{pt}$, its MSE evaluated w.r.t. the pseudotrue parameters is expected to asymptotically converge to the corresponding MCRB. A representative GPS L1 C/A navigation signal is considered, sampled at 8 MHz for 4ms with a single multipath. The MML MSE is obtained from 2000 Monte Carlo runs, for different SNR values. The SNR is defined at the output of the matched filter w.r.t. the LOS source, $\mathrm{SNR}_{\mathrm{out}} = \frac{\rho_0^2\mathbf{s}^H\mathbf{s}}{\sigma_n^2}$. The true parameters values are gathered in Table A.1, where the last column was obtained by running a noiseless simulation. Since the MML is known to be misspecified-unbiased, the estimated parameters in the noiseless case directly correspond to the pseudotrue parameters.

Two RMSEs are computed, one w.r.t. the true parameters and the other one w.r.t. the pseudotrue parameters, which are defined for the $i$-th element of the parameters' vector $\boldsymbol{\theta}$ as follows,

$$\mathrm{RMSE}([\boldsymbol{\theta}_0]_i) \triangleq E\left\{\left([\widehat{\boldsymbol{\theta}}]_i - [\boldsymbol{\theta}_0]_i\right)^2\right\},\ \mathrm{RMSE}([\boldsymbol{\theta}_{pt}]_i) \triangleq E\left\{\left([\widehat{\boldsymbol{\theta}}]_i - [\boldsymbol{\theta}_{pt}]_i\right)^2\right\}, \tag{22}$$

In addition, the bias induced by the model mismatch is also displayed in the results, which is defined for any element $i$ of the parameters' vector $\boldsymbol{\theta}$ as $\text{bias}([\boldsymbol{\theta}]_i) = [\boldsymbol{\theta}_{pt}]_i - [\boldsymbol{\theta}_0]_i$. Finally, the MCRBs are compared to the dual source CRBs corresponding to the true signal model (5), which were derived in [11].

### *5.2. Results*

Figures A.1, A.2, A.3, A.4 show the RMSEs (22) for each of the MML estimates: $\tau$, $F_d = bF_c$, $\rho$ and $\phi$, w.r.t. the true and pseudotrue parameters, which are displayed along with i) their corresponding square-root MCRBs (9), ii) the bias induced by the multipath, and iii) the dual source CRB for the corresponding LOS parameter estimation (i.e., 2S-$\sqrt{\text{CRB}}$).

First, notice that in all the figures, the MML estimators' RMSE w.r.t. the pseudotrue parameters converges to the proposed MCRBs when the SNR gets large enough, which is in accordance with the theory [8]. This proves the validity and exactness of the new MCRBs derived in this contribution, and the asymptotical efficiency of the MML estimator w.r.t. the pseudotrue parameters. Second, the MML estimators' RMSE w.r.t. the true parameters converges to the corresponding $\sqrt{\text{bias}^2 + \text{MCRB}}$, that is, there is a clear performance degradation induced by the bias term, which for large SNR values dominates in front of the MCRB ($\sqrt{\text{bias}^2 + \text{MCRB}} \rightarrow \text{bias}$). A typical GNSS receiver operation point is around SNR=25 dB at the output of the matched filter. For instance, in the case of the time-delay that is the main parameter of interest to solve the positioning problem, in this scenario the performance degradation induced by the multipath is around 4.5m (3m $\rightarrow$ 7.5m). Also, it is interesting to see that the 2S-CRB is above the MCRB for all the estimated parameters: using the MML would then allow the user to get a biased estimate but with a smaller variance. Last point is that the phase estimate is much less impacted by the multipath.

## 6. Conclusion

The multipath effect on the joint delay-Doppler estimation is entirely characterized by the bias term (first order) and MCRB (second order). The multipath-induced biased estimates correspond to the pseudotrue parameters and the resulting lower bound, that differs from the multipath-free scenario, is directly the MCRB. In this study, closed-form MCRB expressions, which only depend on the baseband signal samples, were derived and validated through simulations. This opens the door to a proper ranging-based receiver characterization under multipath conditions, which was a missing theoretical tool in the literature. This bound can be further exploited for signal design and robust estimators derivations for multipath mitigation.

## Acknowledgements

This work was partially supported by CNES and DGA/AID projects 2019.65.0068.00.470.75.01 and 2021.65.0070.00.470.75.01.

## Appendix A. Computation of $\mathbf{A}(\boldsymbol{\theta}_{pt})$

### *Appendix A.1. Model Means Difference Term*

To compute the MCRB, the terms are first considered under their continuous time expression. Then if $a(t;\boldsymbol{\eta}) = s(t-\tau)e^{-j\omega_c b(t-\tau)}$, then

$$\delta a(t) = \alpha_0 a(t;\boldsymbol{\eta}_0) + \alpha_1 a(t;\boldsymbol{\eta}_1) - \alpha_{pt} a(t;\boldsymbol{\eta}_{pt}) = \tilde{\mathbf{A}}(t)\tilde{\boldsymbol{\alpha}}\,, \tag{A.1}$$

$$\tilde{\mathbf{A}}(t) = \left[a(t;\boldsymbol{\eta}_0),\, a(t;\boldsymbol{\eta}_1),\, a(t;\boldsymbol{\eta}_{pt})\right]\,,\ \tilde{\boldsymbol{\alpha}} = \left(\rho_0 e^{j\phi_0}, \rho_1 e^{j\phi_1}, -\rho_{pt} e^{j\phi_{pt}}\right)^T\,. \tag{A.2}$$

Therefore, the discrete expression of this model mismatch term is as: $\delta\mathbf{a} = \tilde{\mathbf{A}}\tilde{\boldsymbol{\alpha}} = \left[\mathbf{a}_0,\, \mathbf{a}_1,\, \mathbf{a}_{pt}\right]\tilde{\boldsymbol{\alpha}}$.

### *Appendix A.2. Differential Terms*

Keeping the continuous time expression for the computation of the successive derivatives, one can easily obtain the first derivative, $\frac{\partial \alpha a(t;\boldsymbol{\eta})}{\partial \boldsymbol{\theta}} = \mathbf{Q}\mathcal{D}^{(1)}(t,\tau)e^{-j\omega_c b(t-\tau)}$, with

$$\mathbf{Q} = \begin{bmatrix} j\alpha\omega_c b & 0 & -\alpha \\ 0 & -j\alpha\omega_c & 0 \\ e^{j\phi} & 0 & 0 \\ \alpha & 0 & 0 \end{bmatrix},\ \mathcal{D}^{(1)}(t;\tau) = \begin{bmatrix} s(t-\tau) \\ (t-\tau)s(t-\tau) \\ s^{(1)}(t-\tau) \end{bmatrix}. \tag{A.3}$$

Similarly the second derivative can be written in a matrix form as,

$$\frac{\partial^2 \alpha a(t;\boldsymbol{\eta})}{\partial\boldsymbol{\theta}\partial\boldsymbol{\theta}^T} = \begin{bmatrix} \mathbf{Q}_1 & \mathbf{Q}_2 & \mathbf{Q}_3 & \mathbf{Q}_4 \end{bmatrix}\left(\mathcal{D}^{(2)}(t;\boldsymbol{\eta}) \otimes \mathbf{I}_4\right) e^{-j\omega_c b(t-\tau)}, \tag{A.4}$$

with

$$\mathbf{Q}_1 = \begin{bmatrix} -\alpha\omega_c^2 b^2 & 0 & 0 & -j2\alpha\omega_c b & 0 & \alpha \\ j\alpha\omega_c & \alpha\omega_c^2 b & 0 & 0 & j\alpha\omega_c & 0 \\ je^{j\phi}\omega_c b & 0 & 0 & -e^{j\phi} & 0 & 0 \\ -\alpha\omega_c b & 0 & 0 & -j\alpha & 0 & 0 \end{bmatrix}, \tag{A.5}$$

$$\mathbf{Q}_2 = \begin{bmatrix} j\alpha\omega_c & \alpha\omega_c^2 b & 0 & 0 & j\alpha\omega_c & 0 \\ 0 & 0 & -\alpha\omega_c^2 & 0 & 0 & 0 \\ 0 & -je^{j\phi}\omega_c & 0 & 0 & 0 & 0 \\ 0 & \alpha\omega_c & 0 & 0 & 0 & 0 \end{bmatrix}, \mathbf{Q}_3 = \begin{bmatrix} je^{j\phi}\omega_c b & 0 & 0 & -e^{j\phi} & 0 & 0 \\ 0 & -je^{j\phi}\omega_c & 0 & 0 & 0 & 0 \\ 0 & 0 & 0 & 0 & 0 & 0 \\ je^{j\phi} & 0 & 0 & 0 & 0 & 0 \end{bmatrix}, \tag{A.6}$$

$$\mathbf{Q}_4 = \begin{bmatrix} -\alpha\omega_c b & 0 & 0 & -j\alpha & 0 & 0 \\ 0 & \alpha\omega_c & 0 & 0 & 0 & 0 \\ je^{j\phi} & 0 & 0 & 0 & 0 & 0 \\ -\alpha & 0 & 0 & 0 & 0 & 0 \end{bmatrix}, \mathcal{D}^{(2)}(t;\tau) = \begin{bmatrix} s(t-\tau) \\ (t-\tau)s(t-\tau) \\ (t-\tau)^2 s(t-\tau) \\ s^{(1)}(t-\tau) \\ (t-\tau)s^{(1)}(t-\tau) \\ s^{(2)}(t-\tau) \end{bmatrix} = \begin{bmatrix} d_1(t) \\ d_2(t) \\ d_3(t) \\ d_4(t) \\ d_5(t) \\ d_6(t) \end{bmatrix}. \tag{A.7}$$

A way to write this Hessian matrix under its discrete form is,

$$\left[\frac{\partial^2 \alpha \mathbf{a}^T}{\partial \boldsymbol{\theta} \partial \boldsymbol{\theta}^T}\right]_{p,q} = \frac{\partial^2 \alpha \mathbf{a}^T}{\partial \theta_p \partial \theta_q} = \left[\mathbf{Q}_q\right]_{p,.} \left[\ldots, \mathcal{D}^{(2)}(nT_s;\boldsymbol{\eta}) e^{-j\omega_c b(nT_s-\tau)}, \ldots\right]_{N_1 \leq n \leq N_2}, \tag{A.8}$$

where $\left[\mathbf{Q}_q\right]_{p,.}$ is the $p$-th row of the matrix $\mathbf{Q}_q$.

*Appendix A.3. Integrals Computation*

The first term of the information matrix $\mathbf{A}(\boldsymbol{\theta}_{pt})$ is simply the product of the model means difference term and the Hessian matrix, which can be expressed element-wise as

$$\delta \mathbf{a}^H \left[\frac{\partial^2 \alpha \mathbf{a}}{\partial \boldsymbol{\theta} \partial \boldsymbol{\theta}^T}\right]_{p,q} = \left(\tilde{\mathbf{A}}\tilde{\boldsymbol{\alpha}}\right)^H \left(\left[\mathbf{Q}_q\right]_{p,.} \left[\ldots, \mathcal{D}^{(2)}(nT_s;\boldsymbol{\eta}) e^{-j\omega_c b(nT_s-\tau)}, \ldots\right]_{N_1 \leq n \leq N_2}\right)^T \tag{A.9}$$

$$= \left[\mathbf{Q}_q\right]_{p,.} \sum_{k \in \{0,1,pt\}} \tilde{\alpha}_k^* \sum_{n=N_1}^{N_2} \begin{bmatrix} a(nT_s;\boldsymbol{\eta}_k)^* d_1(nT_s) e^{-j\omega_c b(nT_s-\tau)} \\ a(nT_s;\boldsymbol{\eta}_k)^* d_2(nT_s) e^{-j\omega_c b(nT_s-\tau)} \\ a(nT_s;\boldsymbol{\eta}_k)^* d_3(nT_s) e^{-j\omega_c b(nT_s-\tau)} \\ a(nT_s;\boldsymbol{\eta}_k)^* d_4(nT_s) e^{-j\omega_c b(nT_s-\tau)} \\ a(nT_s;\boldsymbol{\eta}_k)^* d_5(nT_s) e^{-j\omega_c b(nT_s-\tau)} \\ a(nT_s;\boldsymbol{\eta}_k)^* d_6(nT_s) e^{-j\omega_c b(nT_s-\tau)} \end{bmatrix}. \tag{A.10}$$

Each term of the column vector is then a sum that can be seen as an integral when the number of samples tends to infinity, $\lim_{(N_1,N_2)\to(-\infty,+\infty)} T_s \sum_{n=N_1}^{N_2} a(nT_s;\boldsymbol{\eta}_k)^* d_i(nT_s) e^{-j\omega_c b(nT_s-\tau)} = \int_{\mathbb{R}} a(t;\boldsymbol{\eta}_k)^* d_l(t) e^{-j\omega_c b(t-\tau)} \mathrm{d}t$, therefore, $\lim_{(N_1,N_2)\to(-\infty,+\infty)} \delta \mathbf{a}^H \left[\frac{\partial^2 \alpha \mathbf{a}}{\partial \boldsymbol{\theta} \partial \boldsymbol{\theta}^T}\right]_{p,q} = F_s \left[\mathbf{Q}_q\right]_{p,.} \sum_{k \in \{0,1,pt\}} \tilde{\alpha}_k^* \mathbf{w}^{\mathbf{A}}(\boldsymbol{\eta}_k)$. Finally, thanks to the Shannon Theorem for band-limited signals, the computation of the matrix $\mathbf{A}(\boldsymbol{\theta}_{pt})$ and then of the MCRB reduces to the six following integrals, for $k \in \{0, 1, pt\}$,

$$w_1^{\mathbf{A}}(\boldsymbol{\eta}_k) = \int_{\mathbb{R}} s(t-\tau_{pt}) s(t-\tau_k)^* e^{-j\omega_c \left(b_{pt}(t-\tau_{pt}) - b_k(t-\tau_k)\right)} \mathrm{d}t, \tag{A.11}$$

$$w_2^{\mathbf{A}}(\boldsymbol{\eta}_k) = \int_{\mathbb{R}} (t-\tau_{pt}) s(t-\tau_{pt}) s(t-\tau_k)^* e^{-j\omega_c \left(b_{pt}(t-\tau_{pt}) - b_k(t-\tau_k)\right)} \mathrm{d}t, \tag{A.12}$$

$$w_3^{\mathbf{A}}(\boldsymbol{\eta}_k) = \int_{\mathbb{R}} (t-\tau_{pt})^2 s(t-\tau_{pt}) s(t-\tau_k)^* e^{-j\omega_c \left(b_{pt}(t-\tau_{pt}) - b_k(t-\tau_k)\right)} \mathrm{d}t, \tag{A.13}$$

$$w_4^{\mathbf{A}}(\boldsymbol{\eta}_k) = \int_{\mathbb{R}} s^{(1)}(t-\tau_{pt}) s(t-\tau_k)^* e^{-j\omega_c \left(b_{pt}(t-\tau_{pt}) - b_k(t-\tau_k)\right)} \mathrm{d}t, \tag{A.14}$$

$$w_5^{\mathbf{A}}(\boldsymbol{\eta}_k) = \int_{\mathbb{R}} (t-\tau_{pt}) s^{(1)}(t-\tau_{pt}) s(t-\tau_k)^* e^{-j\omega_c \left(b_{pt}(t-\tau_{pt}) - b_k(t-\tau_k)\right)} \mathrm{d}t, \tag{A.15}$$

$$w_6^{\mathbf{A}}(\boldsymbol{\eta}_k) = \int_{\mathbb{R}} s^{(2)}(t-\tau_{pt}) s(t-\tau_k)^* e^{-j\omega_c \left(b_{pt}(t-\tau_{pt}) - b_k(t-\tau_k)\right)} \mathrm{d}t, \tag{A.16}$$

These integrals are further developed and expressed w.r.t. the baseband samples in [16], which leads to the results in (16)-(21). To compute them, the following elements are involved,

$$\mathbf{s} = \left(\ldots, s(nT_s), \ldots\right)^T_{N_1 \leq n \leq N_2}, \ \boldsymbol{\nu}(f) = \left(\ldots, e^{j2\pi f n}, \ldots\right)^T_{N_1 \leq n \leq N_2}, \tag{A.17}$$

$$\mathbf{U}(p) = \mathrm{diag}\left(\ldots,\, e^{-j2\pi pn},\, \ldots\right)_{N_1 \le n \le N_2},\ \mathbf{D} = \mathrm{diag}\left(\ldots,\, n,\, \ldots\right)_{N_1 \le n \le N_2}, \tag{A.18}$$

$$\mathbf{V}^{\Delta,0}(q) = \int_{-\frac{1}{2}}^{\frac{1}{2}} \boldsymbol{\nu}(f)\boldsymbol{\nu}^H(f)e^{-j2\pi fq}\mathrm{d}f,\ \mathbf{V}^{\Delta,1}(q) = j2\pi \int_{-\frac{1}{2}}^{\frac{1}{2}} f\boldsymbol{\nu}(f)\boldsymbol{\nu}^H(f)e^{-j2\pi fq}\mathrm{d}f, \tag{A.19}$$

$$\mathbf{V}^{\Delta,2}(q) = 4\pi^2 \int_{-\frac{1}{2}}^{\frac{1}{2}} f^2\boldsymbol{\nu}(f)\boldsymbol{\nu}^H(f)e^{-j2\pi fq}\mathrm{d}f. \tag{A.20}$$

## References


[1] H. L. Van Trees, Part III: Radar-Sonar Signal Processing and Gaussian Signals in Noise, Detection, Estimation, and Modulation Theory, Wiley, 2001.

[2] P. J. G. Teunissen, O. Montenbruck (Eds.), Handbook of Global Navigation Satellite Systems, Springer, Switzerland, 2017.

[3] P. J. Huber, The Behavior of Maximum Likelihood Estimates Under Nonstandard Conditions, in: Proc. 5th Berkley Symp. Math. Statist. Probab., 1967, pp. 221–233.

[4] H. Akaike, A New Look at the Statistical Model Identification, IEEE Transactions on Automatic Control 19 (6) (1974) 716–723. doi:10.1109/TAC.1974.1100705.

[5] H. White, Maximum Likelihood Estimation of Misspecified Models, Econometrica: Journal of the Econometric Society (1982) 1–25.

[6] C. D. Richmond, L. L. Horowitz, Parameter Bounds on Estimation Accuracy Under Model Misspecification, IEEE Transactions on Signal Processing 63 (9) (2015) 2263–2278. doi:10.1109/TSP.2015.2411222.

[7] S. Fortunati, F. Gini, M. S. Greco, C. D. Richmond, Performance Bounds for Parameter Estimation under Misspecified Models: Fundamental Findings and Applications, IEEE Signal Processing Magazine 34 (6) (2017) 142–157. doi:10.1109/MSP.2017.2738017.

[8] Q. Ding, S. Kay, Maximum Likelihood Estimator Under a Misspecified Model With High Signal-to-Noise Ratio, IEEE Transactions on Signal Processing 59 (8) (2011) 4012–4016. doi:10.1109/TSP.2011.2150220.

[9] S. F. Yau, Y. Bresler, A Compact Cramér-Rao Bound Expression for Parametric Estimation of Superimposed Signals, IEEE Transactions on Signal Processing 40 (5) (1992) 1226–1230. doi:10.1109/78.134484.

[10] D. Medina, L. Ortega, J. Vilà-Valls, P. Closas, F. Vincent, E. Chaumette, A New Compact CRB for Delay, Doppler and Phase Estimation - Application to GNSS SPP & RTK Performance Characterization, IET Radar, Sonar & Navigationdoi:10.1049/iet-rsn.2020.0168.

[11] C. Lubeigt, L. Ortega, J. Vilà-Valls, L. Lestarquit, E. Chaumette, Joint Delay-Doppler Estimation Performance in a Dual Source Context, Remote Sensing 12 (23) (2020) 3894. doi:10.3390/rs12233894.

[12] U.S. Goverment, Interface Specification IS-GPS-200 Navstar GPS Space/Segment/Navigation User Interface, Tech. rep. (2019).

[13] D. W. Ricker, Echo Signal Processing, Kluwer Academic, Springer, New York, USA, 2003.

[14] B. Ottersten, M. Viberg, P. Stoica, A. Nehorai, Exact and Large Sample Maximum Likelihood Techniques for Parameter Estimation and Detection in Array Processing, in: S. Haykin, J. Litva, T. J. Shepherd (Eds.), Radar Array Processing, Springer-Verlag, Heidelberg, 1993, Ch. 4, pp. 99–151.

[15] E. Kaplan, C. Hegarty, Understanding GPS/GNSS: Principle and Applications, 3rd Edition, Artech House, 2017.

[16] C. Lubeigt, L. Ortega, J. Vilà-Valls, E. Chaumette, Developments for MCRB Computation in Multipath Scenarios, Tech. rep. (2022).

Table A.1: Simulation settings for GPS L1 C/A signal

| | $\boldsymbol{\theta}_0$ | $\boldsymbol{\theta}_1$ | $\boldsymbol{\theta}_{pt}$ |
|---|---|---|---|
| $\tau$ [C/A chip] | 0 | 0.25 | 0.0238 |
| $F_d$ [Hz] | 0 | 100 | 24 |
| $\rho$ [-] | 1 | 0.5 | 1.2342 |
| $\phi$ [rad] | 0 | 0.2618 | 0.0351 |

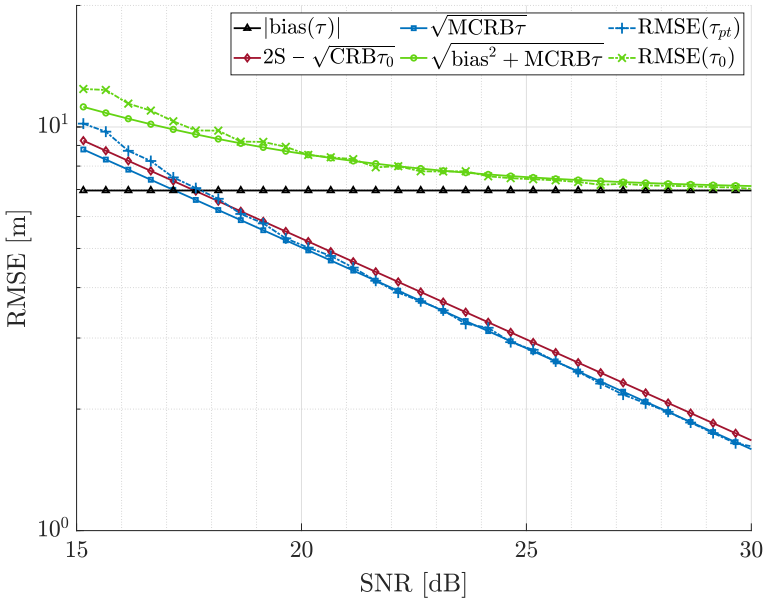


Figure A.1: MML estimator RMSE for time-delay $\tau$ w.r.t. true and pseudotrue parameters, and the corresponding bounds. The results are converted in meters by multiplying them by the speed of light.

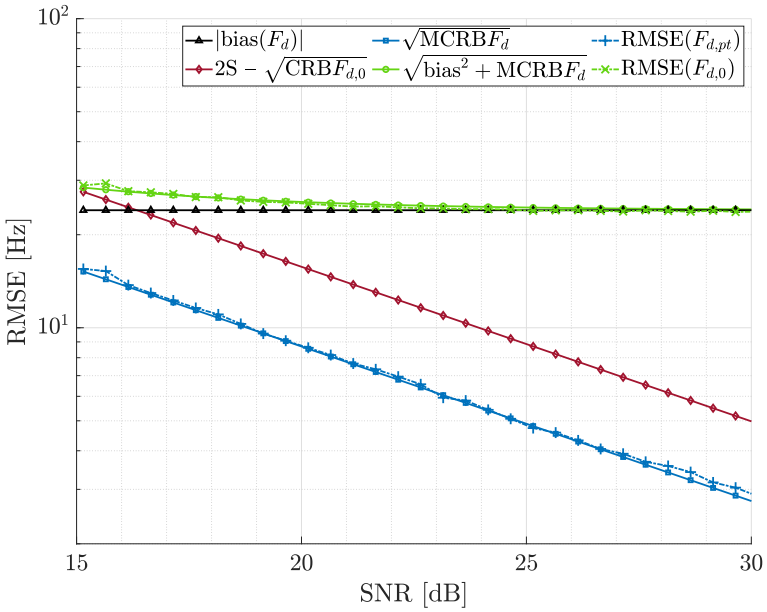


Figure A.2: MML estimator RMSE for Doppler $\boldsymbol{F_d}$ w.r.t. true and pseudotrue parameters, and the corresponding bounds.

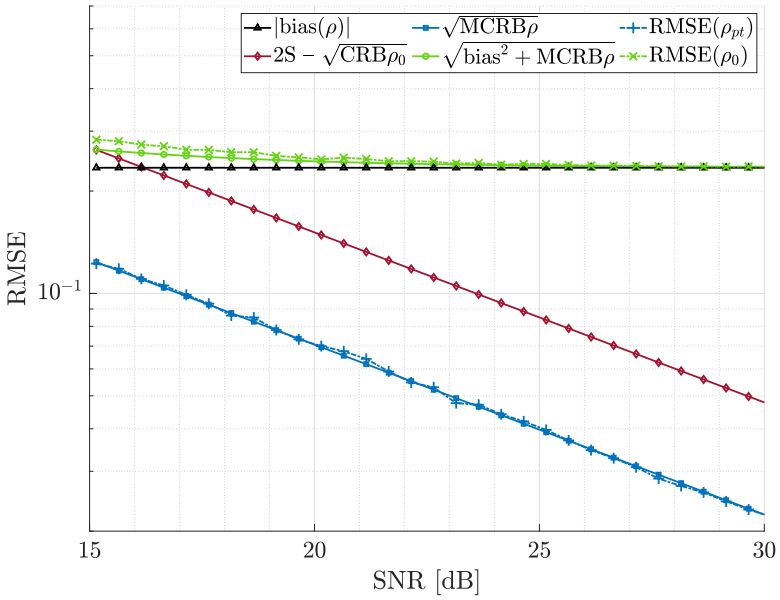


Figure A.3: MML estimator RMSE for amplitude $\rho$ w.r.t. true and pseudotrue parameters, and the corresponding bounds.

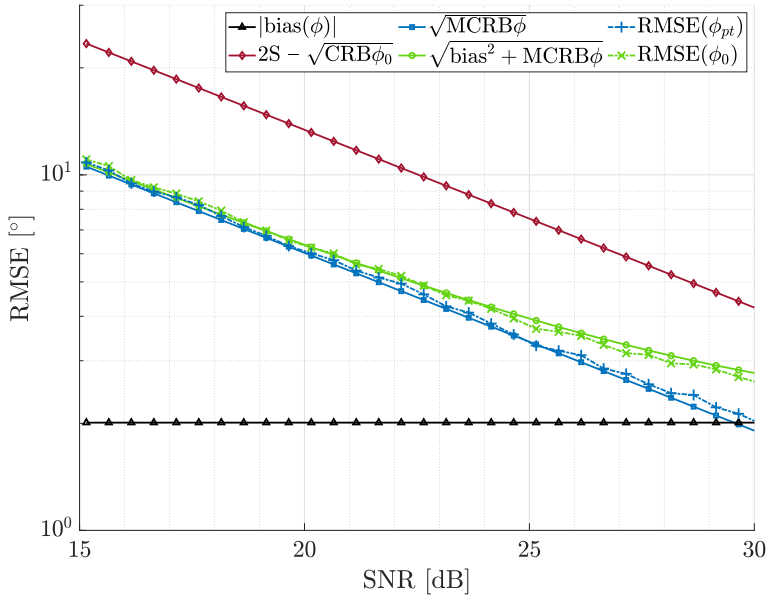


Figure A.4: MML estimator RMSE for phase $\boldsymbol{\phi}$ w.r.t. true and pseudotrue parameters, and the corresponding bounds.